ACS APPLIED MATERIALS & INTERFACES

Research Article

www.acsami.org

In Situ Formation of a Biocatalytic Alginate Membrane by Enhanced Concentration Polarization

Fauziah Marpani,[†,‡] Jianquan Luo,[†,∥] Ramona Valentina Mateiu,[§] Anne S. Meyer,[†] and Manuel Pinelo*[,†]

[†]Department of Chemical and Biochemical Engineering, Center for BioProcess Engineering, Technical University of Denmark, Building 229, DK-2800 Kongens Lyngby, Denmark

[‡]Faculty of Chemical Engineering, Universiti Teknologi MARA, 40450 Shah Alam, Selangor Darul Ehsan, Malaysia

[§]Center for Electron Nanoscopy, Technical University of Denmark, Fysikvej-Building 307, First Floor and Building 314, DK 2800 Kongens Lyngby, Denmark

Supporting Information

ABSTRACT: A thin alginate layer induced on the surface of a commercial polysulfone membrane was used as a matrix for noncovalent immobilization of enzymes. Despite the expected decrease of flux across the membrane resulting from the coating, the initial hypothesis was that such a system should allow high immobilized enzyme loadings, which would benefit from the decreased flux in terms of increased enzyme/substrate contact time. The study was performed in a sequential fashion: first, the most suitable types of alginate able to induce a very thin, sustainable gel layer by pressure-driven membrane filtration were selected and evaluated. Then, an efficient method to make the gel layer adhere to the surface of the membrane was developed. Finally, and after confirming that the enzyme loading could remarkably be enhanced by using this method, several strategies to increase the permeate flux were evaluated. Alcohol dehydrogenase (EC 1.1.1.1), able to catalyze the conversion of formaldehyde into methanol, was selected as the model enzyme. An enzyme loading of 71.4% (44.8 $\mu g/cm^2$) was attained under the optimal immobilization conditions, which resulted in a 40% conversion to methanol as compared to the control setup (without alginate) where only 10.8% (6.9 $\mu g/cm^2$) enzyme was loaded, with less than 5% conversion. Such conversion increased to 60% when polyethylene glycol (PEG) was added during the construction of the gel layer, as a strategy to increase flux. No enzyme leakage was observed for both cases (with/without PEG addition). Modeling results showed that the dominant fouling mechanism during gel layer induction (involving enzyme entrapment) was cake layer formation in the initial and intermediate phases, while pore blocking was the dominant mechanism in the final phase. Such mechanisms had a direct consequence on the type of immobilization promoted in each phase. The results suggested that the strategy proposed could be efficiently used to enhance the enzyme loading on polymer membranes.

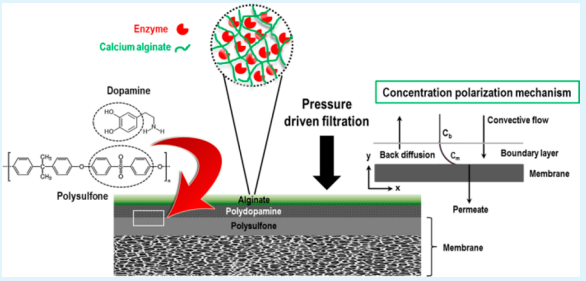

KEYWORDS: *enzymatic membrane reactor, ultrafiltration, membrane fouling, enzyme entrapment, biocatalysis, concentration polarization, polydopamine*

1. INTRODUCTION

Reactive separation technology refers to the coupling of biocatalytic conversion and simultaneous product recovery via filtration. Membrane separation is gaining momentum due to the limited amount of energy required to perform the separation, besides being inexpensive, and the ease of operation and scale-up.[1] In addition, the porous structure of the membrane which can function as a selective barrier as well as a support for enzyme immobilization enables continuous operation and facile product purification and also prevents product inhibition.[2] Enzyme immobilization can furthermore enhance the overall productivity and robustness by improving the reusability and stability of the enzyme, as well as enabling better control of the catalysis process. In an enzymatic membrane reactor (EMR), enzymes can be either free in solution or immobilized in/on the porous structure of the membrane.[3] Either free or immobilized, the presence of enzymes makes membrane separation in EMR prone to fouling. Even though fouling is always seen as an undesirable effect during membrane filtration, recent studies have shown that fouling can be exploited in a positive manner as a strategy to improve enzyme immobilization. Indeed, a correspondence has been found between the mechanisms of enzyme immobilization and the type of fouling promoted during filtration of the enzyme solution.[2]

Alcohol dehydrogenase (ADH) has been previously immobilized in the support layer of a polysulfone membrane following such a technique, resulting in a significantly increased

Received: April 13, 2015
Accepted: July 24, 2015
Published: July 24, 2015

DOI: 10.1021/acsami.5b05529
ACS Appl. Mater. Interfaces 2015, 7, 17682−17691

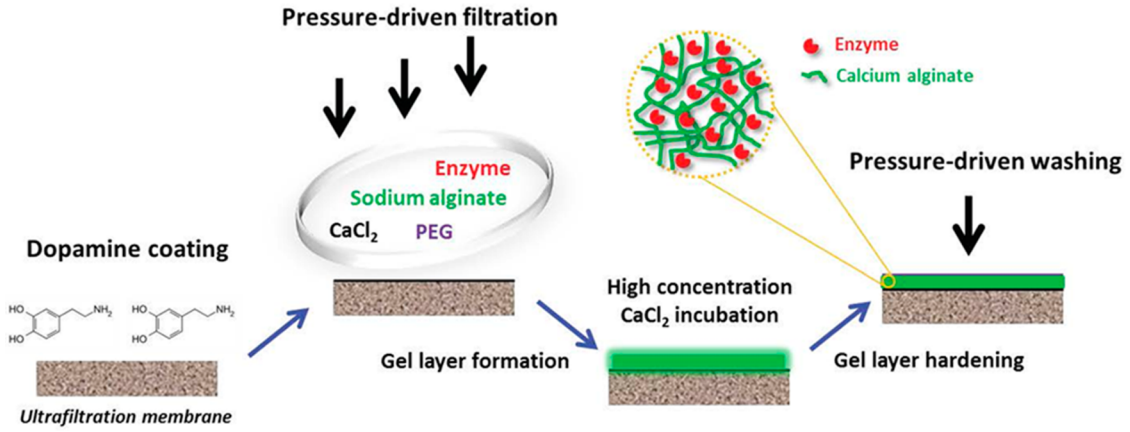

Figure 1. Schematic diagram of *in situ* formation of a biocatalytic alginate membrane by enhanced concentration polarization.

amount of enzyme loading per unit area of the membrane.[4] However, the hydrophobicity of the support layer was found to be unsuitable for the enzyme microenvironment, which resulted in significant losses in activity.[5] Due to its high activity and susceptibility to easily lose such activity under different operation conditions, ADH was used as a model enzyme in this study as well. ADH is an enzyme of particular importance in "cell-factory" processes, e.g., the conversion of carbon dioxide to methanol, in which immobilization could be of crucial importance for the economy and efficiency of the process.[6−12] In the past, several attempts have been made to immobilize ADH, and in all cases, a trade-off was found between the activity and stability of the enzyme.[5] The current work thus aims at solving this dilemma by using the enzyme entrapment concept on an induced, thin, sustainable gel layer of alginate built on top of the membrane skin layer.

Alginate was selected due to its hydrophilicity and biocompatibility with the enzyme microenvironment.[7] The features of the resulting layer of alginate will depend on the ratio of the occurring mannuronic and guluronic acid in the particular type of alginate selected. Filtration of cross-linked alginate, in some way, causes a dilemma between decreasing filtration resistance by formation of aggregates (enhance flux)[13] or increasing reversible/irreversible fouling (flux decline).[14,15] In this work, the alginate gel layer on the membrane was utilized as an immobilization matrix for enzymes. Dopamine was used as a binder between the alginate layer and the membrane material due to 3,4-dihydroxy-L-phenylalanine (dopa) that resembled the glue proteins secreted by marine mussels which can bind strongly to almost all surfaces in aqueous environments.[16] For example, surface modification via self-polymerization of dopamine was successfully demonstrated on halloysite nanotubes providing abundant functional groups to enhance laccase loading for a low-cost and effective enzyme immobilization support.[17]

The hypothesis of the study is that, during the filtration of the alginate−enzyme solution, a particularly high local concentration of alginate will arise near the membrane surface (i.e., concentration polarization phenomenon) and the cross-linking of sodium alginate will slowly occur in the presence of calcium. As a result, the enzymes will be entrapped in the alginate gel layer. Compared to traditional enzyme entrapment in alginate beads,[7] the new strategy is intended to avoid enzyme leakage and overcome the diffusion barrier by membrane sealing and flow-through operation (toward the membrane). This technique is advantageous because enzyme immobilization and concomitant separation of the product can be achieved. To the best of our knowledge, this is the first attempt to immobilize enzyme on a membrane by noncovalent attachment using alginate as the matrix.

2. MATERIALS AND METHODS

2.1. Chemicals, Enzyme, and Membrane. Alcohol dehydrogenase (ADH, EC 1.1.1.1) from *Saccharomyces cerevisiae*, *β*-nicotinamide adenine dinucleotide reduced form (NADH > 97 wt %), formaldehyde, dopamine hydrochloride, alginic acid sodium salt from brown algae, Trizma base, and hydrochloric acid (37%) were purchased from Sigma-Aldrich (St. Louis, MO, USA). The molecular weights of ADH, NADH, and formaldehyde are 141000, 700, and 30 Da, respectively. The buffer used for the enzyme and substrate solution was prepared using 10 mM Tris buffer at pH 7.0. The polysulfone ultrafiltration membrane used in this experiment was from Alfa Laval (GR51PP) with a molecular weight cutoff of 50000 Da.

2.2. Experimental Setup and Procedure. Experiments were conducted in a 50 mL dead-end batch filtration cell (Amicon 8050) from Millipore, Billerica, MA, USA. The cell was fitted with a membrane disc of 44.5 mm in diameter, which resulted in an effective area of 13.4 cm^2. The driving force for this experiment was a constant applied pressure from a nitrogen gas source. The permeate was collected in a beaker on an electronic scale (PJ3000, Mettler, Columbus, OH, USA) or in a precise cylinder to monitor the flux reading. A new membrane was used for each experiment. The virgin membrane was cleaned prior to usage with 70% ethanol for 30 min, following the instructions of the manufacturer, to ensure that all of the pores were wetted. Water permeability was measured afterward at 1 and 2 bar for 20 min. For experiments with the coated membrane, the next step was to coat the membrane with dopamine hydrochloride. A 0.5 g/L amount of dopamine hydrochloride in 10 mM Tris buffer (pH 8.5) was stirred at 100 rpm and exposed to air for 1 h. After that, the polymerization reaction was stopped by washing the membrane thoroughly with deionized water (DI) to ensure that all unreacted dopamine was discarded. A schematic diagram of the experiment is illustrated in Figure 1.

2.2.1. Enzyme Immobilization and Gel Layer Induction. A mixture of 0.05 g/L ADH enzyme, 0.75 g/L alginate, and 10 mM calcium chloride was prepared with Tris buffer at pH 7.0 (polyethylene glycol (PEG) was added in some cases). Gel induction and simultaneous enzyme immobilization were performed by direct dead-end membrane filtration. The permeate was collected in a beaker on an electronic scale. The weight of the permeate collected was recorded every 1 min for the first 20 min and then every 5 min afterward for a maximum of 2 h. After the gel induction/enzyme immobilization, the cell was incubated with 10 mL of 10% $CaCl_2$ solution for 1 h to enhance the rigidity of the induced layer. Finally, the cell was rinsed three times with buffer (5 mL each time) at the end of the filtration, and the final

DOI: 10.1021/acsami.5b05529
ACS Appl. Mater. Interfaces 2015, 7, 17682−17691

retentate and rinsing residuals were collected for enzyme loading calculation. The Bradford method was used to monitor the amount of ADH enzyme immobilized in the feed solution and residues in order to calculate the enzyme loading.

2.2.2. Catalytic Reaction. A 40 mL aliquot of substrate containing 134 μM formaldehyde and 100 μM NADH was poured into the EMR. The quantity of formaldehyde used was in excess to minimize the reverse reaction. A constant pressure of 2 bar was applied until 36 mL (nine aliquots of 4 mL each) of the permeate was obtained. A PerkinElmer lambda 20 UV/vis spectrophotometer (Rodgau, Germany) was used to monitor the NADH concentration by measuring its absorbance at 340 nm.

2.3. Viscosity Measurement. Viscosity measurements of the sodium alginate used in this experiment were conducted using a rapid visco analyzer (RVA-4, Newport Scientific, Warriewood NSW, Australia). Each solution of 3% (w/v) alginate was prepared by mixing a known weight of alginate powder in 50 mL of distilled water. The solution was heated to 50 °C and stirred to facilitate solubilization of the alginate powder. It was then cooled to room temperature before being analyzed.

2.4. Calculated Parameters. The amount of immobilized enzyme was calculated from the mass balance equation:

$$m_i = m_t - C_pV_p - C_rV_r - C_wV_w \quad (1)$$

where m_i and m_t are the immobilized and the total enzyme amounts, respectively; C_p and V_p are the concentration of enzyme in the permeate and the volume of the permeate; C_r and V_r are the enzyme concentration in the retentate and the volume of the retentate; and C_w and V_w are the average enzyme concentration in the rinsing stage and the volume of the washing permeate, respectively.

The immobilization efficiency was expressed as the enzyme loading rate (%):

$$\text{loading rate}/\% = \left(\frac{C_i - C_p}{C_i}\right) \times 100 \quad (2)$$

The conversion rate (%) of formaldehyde to methanol was evaluated from the amount of reduced NADH to NAD^+.

$$\text{conversion rate}/\% = \left(\frac{C_i - C_p}{C_i}\right) \times 100 \quad (3)$$

where C_i and C_p are the NADH concentrations in the feed and permeate, respectively.

3. RESULTS AND DISCUSSION

3.1. Inducing a Stable Alginate Layer on a Polysulfone Membrane. *3.1.1. Different Types of Alginate and the Mechanism of Gelation.* As a first step, the ability of different types of alginate to induce a stable gel layer was evaluated (Table 1). The designation of the types of alginate used (ALG3000G39, ALG2000G67, and ALG200G39) indicate the viscosity (ALG*XXX*), and the guluronic acid content of each type of alginate (G*XX*), which is the group responsible for gelation (Table 1). It was hypothesized that a lower viscosity alginate would induce a more stable, thin layer gel that can "loosely" entrap the enzyme and at the same time permit the substrate to diffuse and react with the enzyme. However, this hypothesis was proven to be wrong, as only the high-viscosity alginates (ALG3000G39 and ALG2000G67) were able to create such a stable layer. Indeed, the gel layers made of ALG3000G39 and ALG2000G67 maintained their integrity throughout the duration of the experiment, whereas the gel formed by ALG200G39 ruptured during the reaction. This was probably the reason for the high conversion rate observed when the ALG200G39 layer was formed. The rupture of the gel made the enzyme leak out from the alginate layer, and the reaction occurred in the bulk solution.

Table 1. Information of Alginate Type Used in the Experiment Obtained from the Manufacturer

product code	mol wt (kDa)	measd viscosity[a] (cP)	*M*:*G* ratio (%)	designation
A2033	80−120	3000	61:39	ALG3000G39
71238	100−200	2000	33:67	ALG2000G67
180947	120−190	200	61:39	ALG200G39

[a]See section 2.3.

Filtration of the alginate−enzyme solution led to severe fouling in a short time. As much as 80% permeate flux reduction (in comparison to clean water flux) was observed after 10 min of filtration in all cases (Figure 2). Previous literature had already shown dramatic decreases in flux during alginate filtration,[14,15] where an alginate solution was also subjected to dead-end filtration in an attempt to mimic the behavior of extracellular polymeric substances in wastewater. In that case, the permeate flux declined more than 90% after 5 min of 325 mg/L alginate filtration.[14] In our case, all types of alginate exhibited the expected trend of permeate flux reduction during filtration, but the reduction depended on the type of alginate. As can be seen, filtration with ALG2000G67 showed the highest permeate flux in the group (Figure 3a). This can be explained considering the content of the respective guluronate (G) and mannuronate (M) residues in the different types of alginate. The G residue content was the highest for ALG2000G67. It is known that the ability of alginate to form a gel is determined by the proportion and length of the G residue in the molecular structure.[18,19] The mechanism of alginate gelation is based on the affinity to bind divalent cations exclusively with the G residue.[20] Interfacial polymerization occurs instantaneously when a sodium alginate solution is mixed with calcium chloride, which results in the formation of calcium alginate aggregates. In this case, it was noticed that the higher the content of G residues in the alginate, the larger the size of the aggregates formed, confirming that G units of the alginate chain have a much higher specificity for calcium binding than M units.[21] The occurrence of aggregates in the formed alginate layer is undesirable, since it makes contact between the substrate and the enzyme more difficult, as the enzyme is confined inside the aggregates. Attempts to break the

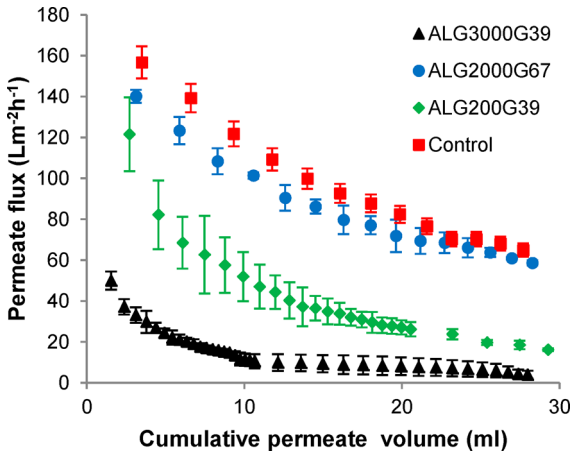

Figure 2. Permeate flux trend during immobilization with different alginates (enzyme immobilized on bare membrane was the control).

DOI: 10.1021/acsami.5b05529
ACS Appl. Mater. Interfaces 2015, 7, 17682−17691

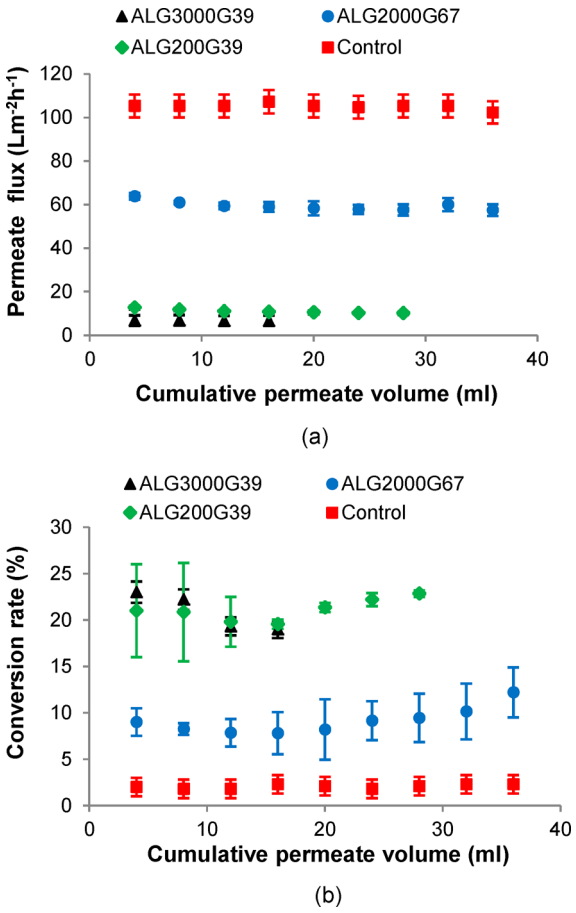

Figure 3. Permeate flux (a) and conversion rate (b) of NADH with various alginate induced reactive membranes during the reaction.

aggregate clumps of ALG2000G67 were conducted using a minivortexer, yet this did not result in a homogenized layer. It was also observed that when the layer was not homogenized (with aggregates), the time taken to filtrate all of the solution will be less (Figure 2). This suggests the water molecules presumably moved more freely toward the membrane surface in this case and subsequently passed through easier than when the alginate layer was more uniform. A study by Fang et al.[22] explained the mechanism for calcium alginate binding. The first phase is when calcium ions interact with single G residue units and form monocomplexes. These monocomplexes will pair up and form egg-box dimers. A dimer refers to two adjacent G residues as well as with two G residues in the opposing chain, which has the capacity to cross-link with Ca^{2+} ions. After egg-box dimers are formed, it will be further associated laterally depending on the proportion of the G and M residues of the alginate. Intercluster association is the mechanism suggested when a high G residue type of alginate is used,[22] which results in a growth of molecular size that may describe the bumps on the surface of the gel induced. The gel structure in this case was mechanically stable with more interstitial spaces that allowed the substrate to pass through more easily, as can be noted in Figure 3a. Thus, during the reaction, the permeate flux was higher with ALG2000G67 in comparison with the low G residues of ALG3000G39 and ALG 200G39.

In the low G residue types of alginate, the lateral association of egg-box dimers is most likely to only happen within an individual cluster because of the greater flexibility and the smaller number of clusters present (due to its high number of M residues). The intracluster association of egg-box dimers is known to cause a reduction in molecular size,[22] which in our case resulted in smaller aggregates. As a result, and in the case of ALG3000G39, the gelation mechanism occurred more evenly to form a flat, compact, smooth-surfaced gel layer. Since the gel formation solution was more homogeneous, the water molecules did not as easily find their way to the membrane surface, which may have partially blocked the membrane pores and became the reason for reduced permeate flux in this case. The progressive process of alginate gelation during filtration was based on the concentration polarization mechanism during which the gel dragged toward the surface of the membrane while pressure was applied. Hydrogen bonding (abundantly available from fractions of G and M residues in alginate molecules) and van der Waals interactions were reported to be the adhesion forces responsible for the gel attachment on the membrane surface.[23] The interaction forces, however, seemed to be too weak to hold the mass of the gel layer and make it stick to the membrane. Indeed, the gel peeled off from the surface of the membrane (Supporting Information Figure S1). This was undesirable because the enzyme, which has been immobilized in the gel, might leak out and be in the free system, resulting in a decrease in enzyme activity.

3.1.2. Dopamine as a Binder between the Alginate Layer and the Membrane Material. To strengthen the adherence between the alginate layer and the membrane material, dopamine was used as an aid. Dopamine contains amine and catechol groups, which can be oxidized in an alkaline environment and can spontaneously cross-link to form a polydopamine structure.[24] The polymer exhibits adhesive properties similar to mussel secretions able to adhere to almost any surface material without needing surface preparation.[24] A recent work from Luo et al.[25] has demonstrated that dopamine can successfully polymerize and adhere on poly(ether sulfone) membrane in solution under mild conditions. In our study, 0.5 g/L dopamine was oxidized in the air, in a stirred cell containing alkaline buffer (pH 8.5) for 60 min. A blackish surface was observed afterward (Figure S2), indicating that dopamine was indeed polymerized on the membrane surface. The blackish surface formation mechanism is similar to the mechanism of melanin formation. A previous study also confirmed that polydopamine polymerization should not chemically degrade or affect the membrane.[26] It is worth mentioning that caffeic acid, which also contains a catechol group, was also used in an attempt to adhere the alginate layer to the membrane, with no success. However, it was observed that the occurrence of catechol contributed to make the membrane more hydrophilic (data not shown).

A detailed understanding of the polymerization mechanism of polydopamine is not known so far, but there have been reported logical explanations for the phenomenon.[27,28] The dissolved oxygen would induce the oxidation of dopamine into a quinone as the first step, leading to polymerization in an aerated alkaline solution. Catechol is easily oxidized to quinone in alkaline solution, and the cross-linking is attributed to the reverse dismutation reaction between the catechol and *o*-quinone forms of the dopamine molecule.[29] The second step involves cyclization of dopaminequinone via 1,4-Michael addition, which leads to the formation of leucodopamine-chrome. Leucodopaminechrome will be in turn oxidized to dopaminechrome and then further be oxidized to 5,6-dihydroxindole. As a result of hydrogen bonding in the

DOI: 10.1021/acsami.5b05529
ACS Appl. Mater. Interfaces 2015, 7, 17682−17691

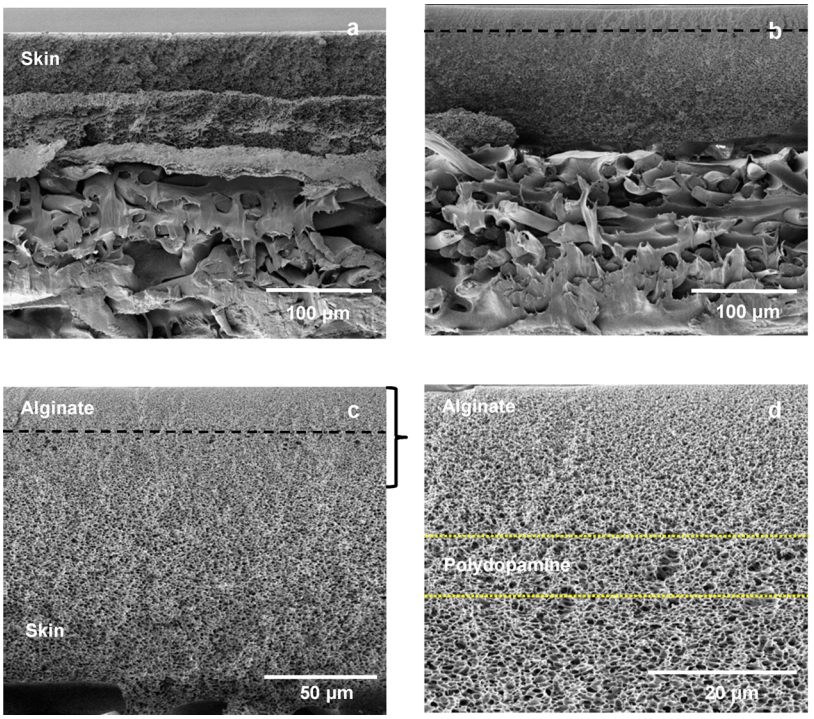

Figure 4. SEM image of membrane cross-section (a), bare polysulfone membrane (b), and polysulfone membrane coated with dopamine (c) and (d) alginate.

catechol group, the monomers of 5,6-dihydroxindole linked together through biphenyl-type bonds by which one envisages a covalent, polymeric skeleton, adsorbed on the surface of the substrate leaving behind a tough hydrophilic coating.[30] The reaction will go on for a certain period of time, after which the dopamine content might be depleted or reach a plateau due to the competition between polydopamine deposition and solubilization.[26] Recently, by using solid-state spectroscopic and crystallographic techniques, the covalent polydopamine structure was re-examined, where a noncovalent, supramolecular aggregate of monomers consisting of 5,6-dihydroxindole and dopaminechrome were suggested to be held together by a combination of charge transfer, π-stacking, and hydrogen bonding interactions.[31] Another study reported the identification of physical, self-assembly trimer of dopamine and dihydroxindole existed in the complex structure of polydopamine via analysis of high-performance liquid chromatography coupled with mass spectrometry.[32]

Figure 4 shows a cross-sectional view of a bare polysulfone membrane and a polysulfone membrane that had been coated with dopamine and alginate. Polysulfone membranes consist of a very thin skin layer that has a molecular weight cutoff specification (50 kDa) and a thicker support layer (fiber-like structure). Dopamine was coated on top of the skin layer in order to subsequently make the alginate layer adhere unto the surface of the membrane. Comparing parts a and b of Figure 4, it can be deduced that the induced alginate layer thickness was approximately 20 μm. By looking at the figure, it can be seen that the pore structure became smaller and more compact (Figure 4c). In between the alginate and the skin layer (Figure 4d), clusters of bigger pores between the small porous layer may indicate the presence of polydopamine. No distinct layer can be observed directly from the SEM images. Nevertheless, using image analysis software, the average pore sizes of the alginate, skin layer, and polydopamine cluster could be estimated to be 200 $\pm$ 50 nm, 1.58 $\pm$ 0.14 μm, and 2.20 $\pm$ 0.34 μm, respectively.

Membrane hydrophilicity may increase or decrease when a membrane surface is modified with a polydopamine coating.[33] In our case, it was important to increase the hydrophilicity in order to ensure an acceptable flux through the membrane. The hydrophilic surface will create a strongly bound water layer which acts as a buffer that can minimize direct foulant-surface interactions and prevent hydrophobic−hydrophobic interactions.[34] Unfortunately, water permeability levels before and after coating with dopamine decreased by around 10%. The reduction of flux was also observed in a previous study, in which the reduction was even greater.[35] During the initial stages of deposition, polydopamine presumably penetrated into the porous structure of the polysulfone membrane due to its low molecular weight. Such deposition would lead to pore constriction and result in decreases of the membrane water permeability.[26] Permeate flux seemed to give the same trend for coated and noncoated membrane surfaces during immobilization (Figure 5).

As can be observed, the conversion rate for ALG3000G39 showed a remarkable increase from 20% to 40% (Figure 6). This is consistent with the amount of enzyme loading shown in Table 2 (71% of the enzyme was loaded in the gel). The increase also may be due to the contact time between the substrate and the enzyme where the permeate flux is lower than ALG2000G67.

3.2. Fouling Mechanism. From observation of the pattern of permeate flux versus time during the immobilization step, an abrupt decline was noted at the initial stage of the filtration (Figure 2). The rate of fouling then decreased at a steady state until a plateau was reached. This is common behavior observed during conventional ultrafiltration at a constant TMP.[36] In this case, the feed solution contained the enzyme, calcium chloride, sodium alginate, and Tris buffer solution. Calcium ions may

DOI: 10.1021/acsami.5b05529
ACS Appl. Mater. Interfaces 2015, 7, 17682−17691

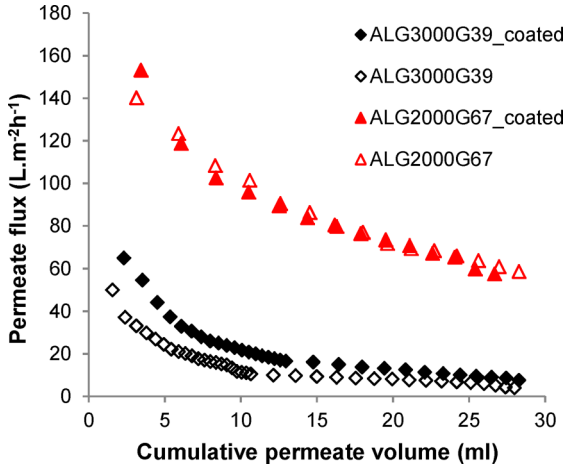

Figure 5. Permeate flux trend during immobilization/gel induction on coated and noncoated membrane (transmembrane pressure (TMP) = 2 bar).

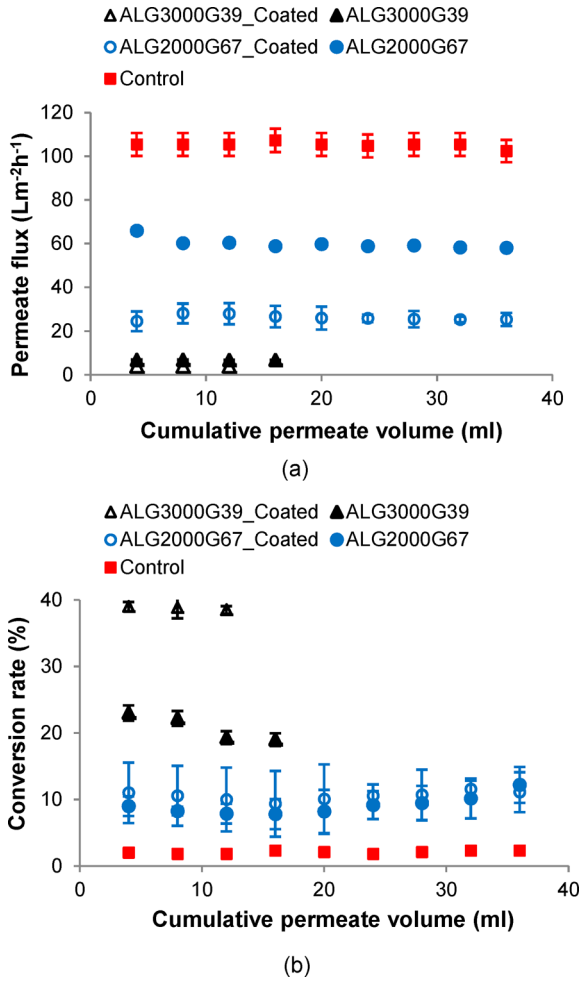

Figure 6. Permeate flux (a) and conversion rate (b) of NADH with various alginates induced on dopamine coated reactive membranes during the reaction.

presumably have completely bound to alginate to form calcium alginate aggregates. During the formation of aggregates, part of the enzyme was probably entrapped with the intercluster/intracluster association of dimers, while some of the enzyme could still be "free" in the solution. When pressure was applied

Table 2. Membrane Permeability and Enzyme Loading for the Reactive Membranes Induced by Different Types of Alginate with Dopamine Coating

	membrane permeability ($L\ m^{-2}\ h^{-1}\ bar^{-1}$)			
alginate type	initial	fouled	enzyme loading ($\mu g\ cm^{-2}$)	loading rate (%)
ALG3000G39	120.0–127.6	3.8 ± 0.06	44.8	71.4
ALG2000G67		28.8 ± 0.68	36.9	58.9
control		32.5 ± 2.63	6.9	10.8

in the reactor, the nonentrapped enzyme was apparently dragged toward the membrane surface. The so-called free enzyme could only block the surface of the membrane pore due to its larger size (141 kDa), in comparison with the membrane pore size (50 kDa). To understand further the fouling mechanisms, the permeate flux curve plotted against time was separated into three phases or time intervals (Figure 7). The

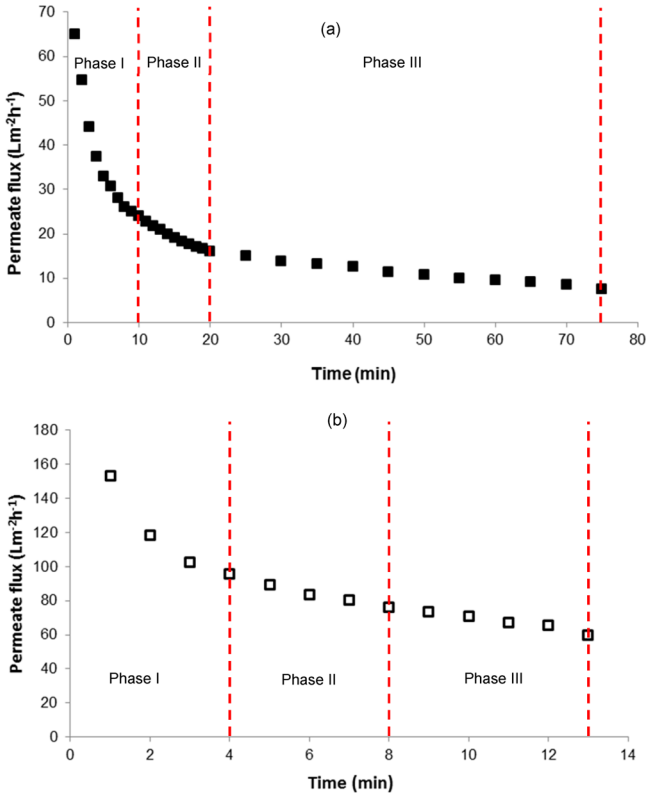

Figure 7. Analysis region of fouling behavior during immobilization by fitting to Hermia's model: (a) ALG3000G39 and (b) ALG2000G67.

difference in the duration of the time intervals on Figure 7a,b was due to the fixed volume that had been set at 30 mL for the feed solution of both types of alginate (section 2). Fitting the results to Hermia's model (Table S1) showed that the fouling mechanism for phase I and II was controlled by cake layer formation, whereas pore blocking dominated the final phase (Table 3). In phase I, the sharp decline at the initial stage of filtration could be attributed to the occurrence of calcium alginate aggregates and free enzyme that accumulated on the bare membrane. Both formed a dense gel layer that reduced the area available for unconstrained filtration, which resulted in

DOI: 10.1021/acsami.5b05529
ACS Appl. Mater. Interfaces 2015, 7, 17682–17691

Table 3. Coefficient of Regression (R^2) of Hermia's Model Fitting for the Separate Regions during Immobilization on the Coated Membrane Surface

alginate type	phase I		phase II		phase III	
ALG3000G39	complete blocking	0.8177	complete blocking	0.993	complete blocking	0.9929
	standard blocking	0.8933	standard blocking	0.9962	standard blocking	0.9887
	intermediate blocking	0.9478	intermediate blocking	0.9983	intermediate blocking	0.9795
	cake layer formation	0.9957	cake layer formation	0.9991	cake layer formation	0.9463
ALG2000G67	complete blocking	0.8999	complete blocking	0.9922	complete blocking	0.9635
	standard blocking	0.9459	standard blocking	0.9936	standard blocking	0.9581
	intermediate blocking	0.9318	intermediate blocking	0.9946	intermediate blocking	0.9522
	cake layer formation	0.9784	cake layer formation	0.9958	cake layer formation	0.9389

increased filtration resistance. As the filtration time progressed, the permeate flux also decreased and the concentration polarization became lower, which resulted in the newly formed, more porous gel layer in phase II. In phase III, the calcium alginate aggregated and the free enzyme probably blocked the porous gel layer, which can be regarded as pore blocking behavior. It was expected that the rate of the permeate flux would depend on the stiffness of the gel network and the amount of enzyme immobilized. In the final phase, the membrane surface became severely fouled due to gel formation, causing an increase in hydraulic resistance to flow.[37] To quantify the cake layer resistance between ALG3000G39- and ALG2000G67-induced layers, the data were fitted to the cake layer model (Figure 8). The slope of the curve showed that the

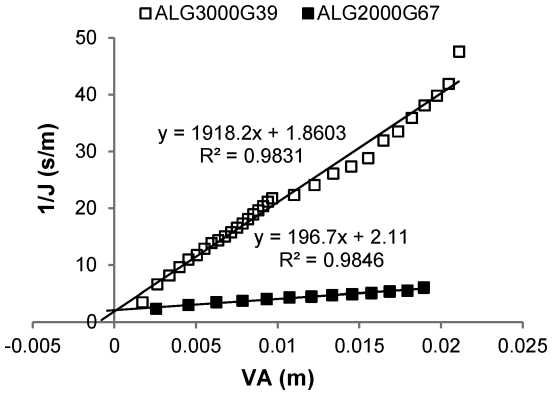

Figure 8. Cake layer model fitting.

cake resistance for ALG3000G39 was higher than for ALG2000G67. The ideal conditions would be higher enzyme loading with less filtration resistance. However, since the highest enzyme loading was recorded with ALG3000G39 (Table 2), this type of alginate was selected for the subsequent study.

3.3. Strategies To Increase Flux. Previous sections showed the advantages of immobilizing ADH in terms of maintaining enzyme activity. Indeed, our data confirmed that the conversion was increased to a value of 40% under the optimal conditions, as compared to the control (Figure 6). However, the immobilization also caused a considerable flux decrease. A few strategies to increase the flux flow were thus attempted in this study. The strategy to attain a flux increase through the alginate layer was to create a more porous layer of alginate with big enough interstices to make possible the exposure of the enzyme active site and also permit the substrate to be in contact with the enzyme. On the other hand, pores should be small enough to avoid enzyme leakage from the network. The strategies included variations in the Ca^{2+} concentrations during alginate layer formation, the addition of PEG into the feed solution, induced gelation with pectin, and induced gelation with mixed types of alginate (1:1 ratio between ALG2000G67 and ALG3000G39). It is worth mentioning that both induced gelation with pectin and mixed alginate types did not help to achieve our purpose (gel layer ruptured or enzyme leakage occurred; data not shown). Therefore, the work continued on the other two strategies.

3.3.1. Effect of the $CaCl_2$ Concentration. The effect of several Ca^{2+} concentrations in the feed (5, 10, and 20 mM) was evaluated. Alginate ALG3000G39 was selected for this experiment, as its use resulted in the highest amount of enzyme loading during immobilization. The results show that cross-linking of alginate with 5 and 20 mM Ca^{2+} led to a nonfavorable structure of the gel network that ruptured, as seen from the increasing trend of permeate flux (Figure 9). Indeed, the gel was observed to swell when a 20 mM Ca^{2+} concentration was used, to subsequently rupture during the reaction. Enzyme leakage was observed with the induction of a gel with 5 mM concentration. Limiting calcium concentration could cause random cross-linking to a certain carboxylate group in the G residue, hence resulting in bigger interstices. It was demonstrated that a high percentage of M residue in ALG3000G39 has the affinity to covalently attach with dopamine coated on the membrane.[38] Bigger interstices in the gel network would allow the enzyme to escape from the entrapment, while covalent attachment between M residue and dopamine would cramp and conform the enzymes, thus restraining exposure of its active sites. Apparently, high M residue type of alginate gelation mechanism follows intracluster association of dimers (section 3.1) and can be easily disrupted by competing ions.[39] Ion exchange process leads to chain relaxation of an egg-box junction dimer and is responsible for the observed swelling of the gel matrix.[40,41] Subsequent stretching due to pressure induced by the penetration of water and salt creates a weakened gel structure that consequently ruptured.[39] Trials with different Ca^{2+} concentrations during gel induction concluded that there is indeed an optimal amount of Ca^{2+} ions needed for an ideal structure of gel network, in terms of both high flux and low enzyme leakage.

3.3.2. Effect of PEG Addition. PEG is widely used as an additive to manipulate pore size during membrane fabrication.[42,43] It also possesses a high degree of biocompatibility and nontoxicity. In this case, the addition of PEG successfully increased the permeate flux through the membrane (Figure 10). The higher the molecular weight of PEG, the higher the permeate flux increased. Nevertheless, the molecular weight was inversely proportional to the conversion rate during the reaction. With PEG1500, the conversion of formaldehyde to

DOI: 10.1021/acsami.5b05529
ACS Appl. Mater. Interfaces 2015, 7, 17682−17691

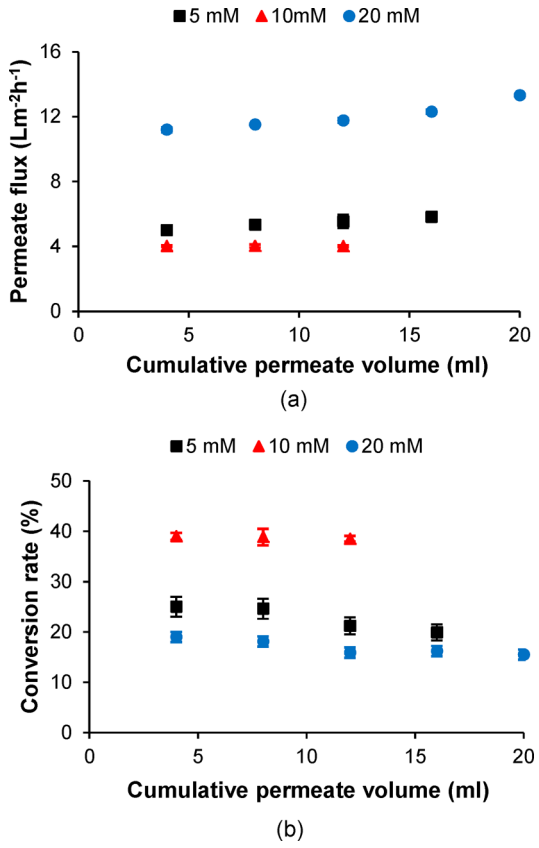

Figure 9. Permeate flux (a) and conversion rate (b) of various biocatalytic membranes induced by different calcium concentrations during the reaction.

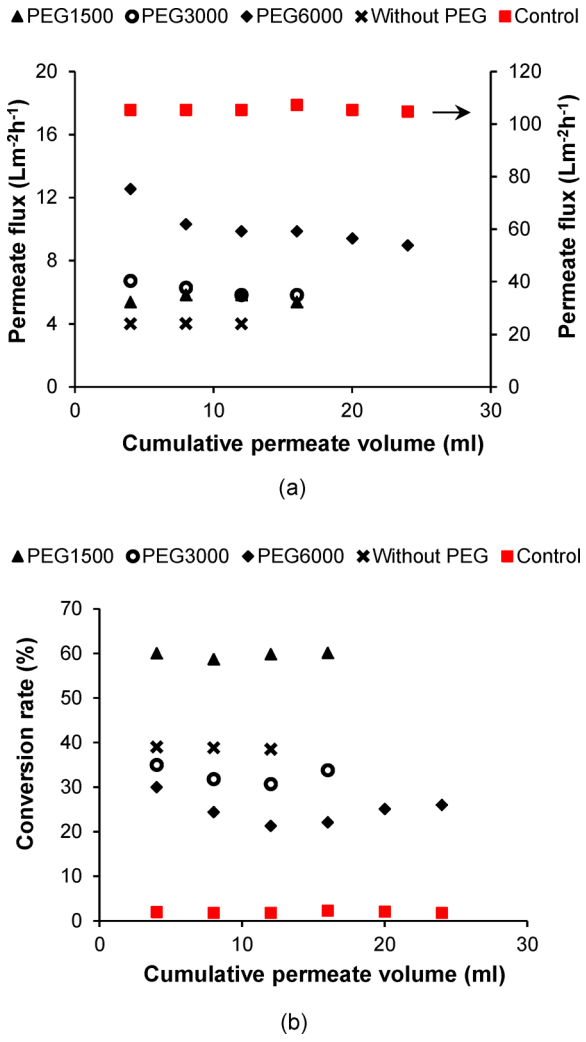

Figure 10. Permeate flux (a) and conversion rate (b) of NADH for various biocatalytic membranes induced with different molecular weights of PEG during the reaction.

methanol significantly increased from 40% (without PEG addition) to 60% and no enzyme leakage was detected. This was a reasonably promising outcome, albeit the permeate flux during reaction did not increase significantly. PEG molecules are believed to prevent/interrupt the cross-linking of intra-cluster association of alginate dimers (section 3.1). In the presence of salt ions (Ca^{2+}), PEG and alginate become immiscible causing the formation of voids filled with PEG.[44] Since the molecular weight (size) of the PEG molecules was relatively smaller than the pore of the membrane, it would be expected that the molecules would diffuse out from the void network during the pressurized washing stage, resulting in some microchannels/-voids in the gel matrix. The phenomenon of low molecular weight of PEG being diffused out from the alginate network is similar to what was deduced by Seifert and Phillips.[44] The occurrence of such channels could increase the exposure of enzyme active sites and thus improve the biocatalytic conversion (Figure 10a). In contrast, swelling of the gel was again observed when the gel was mixed with PEG6000. As a consequence, the immobilized enzyme washed away, causing a low and unstable conversion rate (Figure 10b). The higher permeate flux with PEG6000 addition was simply because the gel had ruptured and detached from the membrane. The physical appearance of gels induced with different molecular weights of PEG can be seen in Figure S3.

4. CONCLUSION

Inevitable fouling associated with membrane separation processes could be exploited as a strategy to immobilize enzymes on the surface of an ultrafiltration membrane by entrapment of the enzyme in a stable, thin calcium alginate gel layer. Technically, concentration polarization was the dominant mechanism that governed the induction of the thin calcium alginate layer and immobilization of the enzyme. It was confirmed that the composition of mannuronic and guluronic acid in alginate determined the features and properties of the gel layer induced on the surface of the membrane. A higher viscosity type of alginate with a low guluronic acid fraction was the most suitable type of alginate in this application. The mussel secretion adhesive compound, polydopamine, coated on the membrane surface prior to gel induction and enzyme immobilization, was found to aid in the gel detachment issue in this study and in a way prevented the gel layer from being destroyed. During this fouling-induced enzyme immobilization process, it could be deduced from Hermia's model that fouling is governed solely by cake layer formation in the initial and intermediate phases and further upgraded to pore blocking in the final phase of filtration. Moreover, a suitable calcium concentration and PEG addition were found to improve biocatalytic layer formation. This strategy had a positive impact as increases in enzyme loading and the conversion rate were reported and, hence, opens a new perspective for developing

DOI: 10.1021/acsami.5b05529
ACS Appl. Mater. Interfaces 2015, 7, 17682−17691

high-performance reactive-separation systems in which a high enzyme loading is required.

■ ASSOCIATED CONTENT

Supporting Information

The Supporting Information is available free of charge on the ACS Publications website at DOI: 10.1021/acsami.5b05529.

Peeled off gel, gel layer induced on dopamine coated membrane, empirical description of fouling model, and gel layer with PEG (PDF)

■ AUTHOR INFORMATION

Corresponding Author

*E-mail: mp@kt.dtu.dk.

Present Address

[‖]National Key Laboratory of Biochemical Engineering (NKLBE), Institute of Process Engineering, Chinese Academy of Sciences, No. 1 N. 2nd St., Zhongguancun, Haidian District, 100190, Beijing, China.

Notes

The authors declare no competing financial interest.

■ ACKNOWLEDGMENTS

F.M. thanks the Ministry of Education Malaysia and Universiti Teknologi MARA for the scholarship award.

■ REFERENCES

(1) Pal, P.; Sikder, J.; Roy, S.; Giorno, L. Process Intensification in Lactic Acid Production: A Review of Membrane Based Processes. *Chem. Eng. Process.* **2009**, *48*, 1549−1559.

(2) Luo, J.; Meyer, A. S.; Jonsson, G.; Pinelo, M. Enzyme Immobilization by Fouling in Ultrafiltration Membranes: Impact of Membrane Configuration and Type on Flux Behavior and Biocatalytic Conversion Efficacy. *Biochem. Eng. J.* **2014**, *83*, 79−89.

(3) Jochems, P.; Satyawali, Y.; Diels, L.; Dejonghe, W. Enzyme Immobilization on/in Polymeric Membranes: Status, Challenges and Perspectives in Biocatalytic Membrane Reactors (BMRs). *Green Chem.* **2011**, *13*, 1609−1623.

(4) Luo, J.; Marpani, F.; Brites, R.; Frederiksen, L.; Meyer, A. S.; Jonsson, G.; Pinelo, M. Directing Filtration to Optimize Enzyme Immobilization in Reactive Membranes. *J. Membr. Sci.* **2014**, *459*, 1−11.

(5) Bolivar, J. M.; Rocha-Martín, J.; Mateo, C.; Guisan, J. M. Stabilization of a Highly Active but Unstable Alcohol Dehydrogenase from Yeast Using Immobilization and Post-immobilization Techniques. *Process Biochem.* **2012**, *47*, 679−686.

(6) Obert, R.; Dave, B. C. Enzymatic Conversion of Carbon Dioxide to Methanol: Enhanced Methanol Production in Silica Sol - Gel Matrices. *J. Am. Chem. Soc.* **1999**, *121*, 12192−12193.

(7) Xu, S.; Lu, Y.; Li, J.; Jiang, Z.; Wu, H. Efficient Conversion of CO_2 to Methanol Catalyzed by Three Dehydrogenases Co-encapsulated in an Alginate - Silica (ALG - SiO_2) Hybrid Gel. *Ind. Eng. Chem. Res.* **2006**, *45*, 4567−4573.

(8) Sun, Q.; Jiang, Y.; Jiang, Z.; Zhang, L.; Sun, X.; Li, J. Green and Efficient Conversion of CO_2 to Methanol by Biomimetic Coimmobilization of Three Dehydrogenases in Protamine-templated Titania. *Ind. Eng. Chem. Res.* **2009**, *48*, 4210−4215.

(9) Shi, J.; Zhang, L.; Jiang, Z. Facile Construction of Multicompartment Multienzyme System through Layer-by-layer Self-assembly and Biomimetic Mineralization. *ACS Appl. Mater. Interfaces* **2011**, *3*, 881−889.

(10) Cazelles, R.; Drone, J.; Fajula, F.; Ersen, O.; Moldovan, S.; Galarneau, A. Reduction of CO_2 to Methanol by a Polyenzymatic System Encapsulated in Phospholipids−silica Nanocapsules. *New J. Chem.* **2013**, *37*, 3721−3730.

(11) Wang, X.; Li, Z.; Shi, J.; Wu, H.; Jiang, Z.; Zhang, W.; Song, X.; Ai, Q. Bioinspired Approach to Multienzyme Cascade System Construction for Efficient Carbon Dioxide Reduction. *ACS Catal.* **2014**, *4*, 962−972.

(12) Luo, J.; Meyer, A. S.; Mateiu, R. V.; Pinelo, M. Cascade Catalysis in Membranes with Enzyme Immobilization for Multi-enzymatic Conversion of CO_2 to Methanol. *New Biotechnol.* **2015**, *32*, 319−327.

(13) Van de Ven, W. J. C.; Sant, K. V.; Pünt, I. G. M.; Zwijnenburg, A.; Kemperman, A. J. B.; Van der Meer, W. G. J.; Wessling, M. Hollow Fiber Dead-end Ultrafiltration: Influence of Ionic Environment on Filtration of Alginates. *J. Membr. Sci.* **2008**, *308*, 218−229.

(14) Chen, D.; Columbia, M. Enzymatic Control of Alginate Fouling of Dead-end MF and UF Ceramic Membranes. *J. Membr. Sci.* **2011**, *381*, 118−125.

(15) Katsoufidou, K.; Yiantsios, S. G.; Karabelas, A. J. Experimental Study of Ultrafiltration Membrane Fouling by Sodium Alginate and Flux Recovery by Backwashing. *J. Membr. Sci.* **2007**, *300*, 137−146.

(16) Lee, H.; Scherer, N. F.; Messersmith, P. B. Single-molecule Mechanics of Mussel Adhesion. *Proc. Natl. Acad. Sci. U. S. A.* **2006**, *103*, 12999−13003.

(17) Chao, C.; Liu, J.; Wang, J.; Zhang, Y.; Zhang, B.; Zhang, Y.; Xiang, X.; Chen, R. Surface Modification of Halloysite Nanotubes with Dopamine for Enzyme Immobilization. *ACS Appl. Mater. Interfaces* **2013**, *5*, 10559−10564.

(18) Donati, I.; Paoletti, S. Material Properties of Alginates. In *Alginates: Biology and Applications*; Rehm, B. H. A., Ed.; Springer-Verlag: Berlin, Germany, 2009; pp 1−53.

(19) Draget, K. I.; Skjåk-Braek, G.; Smidsrød, O. Alginate Based New Materials. *Int. J. Biol. Macromol.* **1997**, *21*, 47−55.

(20) Davidovich-Pinhas, M.; Bianco-Peled, H. A Quantitative Analysis of Alginate Swelling. *Carbohydr. Polym.* **2010**, *79*, 1020−1027.

(21) Braccini, I.; Pérez, S. Molecular Basis of Ca^{2+} - Induced Gelation in Alginates and Pectins: The Egg-box Model Revisited. *Biomacromolecules* **2001**, *2*, 1089−1096.

(22) Fang, Y.; Al-Assaf, S.; Phillips, G. O.; Nishinari, K.; Funami, T.; Williams, P. A.; Li, L. Multiple Steps and Critical Behaviors of the Binding of Calcium to Alginate. *J. Phys. Chem. B* **2007**, *111*, 2456−2462.

(23) Xiang, Y.; Liu, Y.; Mi, B.; Leng, Y. Molecular Dynamics Simulations of Polyamide Membrane, Calcium Alginate Gel and Their Interactions in Aqueous Solution. *Langmuir* **2014**, *30*, 9098−9106.

(24) Lee, H.; Dellatore, S. M.; Miller, W. M.; Messersmith, P. B. Mussel-inspired Surface Chemistry for Multifunctional Coatings. *Science* **2007**, *318*, 426−430.

(25) Luo, J.; Meyer, A. S.; Mateiu, R. V.; Kalyani, D.; Pinelo, M. Functionalization of a Membrane Sublayer using Reverse Filtration of Enzymes and Dopamine Coating. *ACS Appl. Mater. Interfaces* **2014**, *6*, 22894−22904.

(26) McCloskey, B. D.; Park, H. B.; Ju, H.; Rowe, B. W.; Miller, D. J.; Chun, B. J.; Kin, K.; Freeman, B. D. Influence of Polydopamine Deposition Conditions on Pure Water Flux and Foulant Adhesion Resistance of Reverse Osmosis, Ultrafiltration, and Microfiltration Membranes. *Polymer* **2010**, *51*, 3472−3485.

(27) Messersmith, P. B.; Black, I. K. C. L.; Yi, J.; Rivera, J. G. Multifunctional Metal Nanoparticles Having a Polydopamine-Based Surface and Methods of Making and Using the Same. U.S. Patent 20120237605 A1, Sep. 20, 2012.

(28) Dreyer, D. R.; Miller, D. J.; Freeman, B. D.; Paul, D. R.; Bielawski, C. W. Perspectives on Poly(dopamine). *Chem. Sci.* **2013**, *4*, 3796−3802.

(29) Li, B.; Liu, W.; Jiang, Z.; Dong, X.; Wang, B.; Zhong, Y. Ultrathin and Stable Active Layer of Dense Composite Membrane Enabled by Poly(dopamine). *Langmuir* **2009**, *25*, 7368−7374.

(30) Della Vecchia, N. F.; Avolio, R.; Alfè, M.; Errico, M. E.; Napolitano, A.; d'Ischia, M. Building-Block Diversity in Polydopamine Underpins a Multifunctional Eumelanin-Type Platform Tunable Through a Quinone Control Point. *Adv. Funct. Mater.* **2013**, *23*, 1331−1340.

DOI: 10.1021/acsami.5b05529
ACS Appl. Mater. Interfaces 2015, 7, 17682−17691

(31) Dreyer, D. R.; Miller, D. J.; Freeman, B. D.; Paul, D. R.; Bielawski, C. W. Elucidating the Structure of Poly(dopamine). *Langmuir* **2012**, *28*, 6428−6435.
(32) Hong, S.; Na, Y. S.; Choi, S.; Song, I. T.; Kim, W. Y.; Lee, H. Non-covalent Self-assembly and Covalent Polymerization Co-contribute to Polydopamine Formation. *Adv. Funct. Mater.* **2012**, *22*, 4711−4717.
(33) Arena, J. T.; McCloskey, B.; Freeman, B. D.; McCutcheon, J. R. Surface Modification of Thin Film Composite Membrane Support Layers with Polydopamine: Enabling Use of Reverse Osmosis Membranes in Pressure Retarded Osmosis. *J. Membr. Sci.* **2011**, *375*, 55−62.
(34) Vrijenhoek, E. M.; Hong, S.; Elimelech, M. Influence of Membrane Surface Properties on Initial Rate of Colloidal Fouling of Reverse Osmosis and Nanofiltration Membranes. *J. Membr. Sci.* **2001**, *188*, 115−128.
(35) Li, F.; Meng, J.; Ye, J.; Yang, B.; Tian, Q.; Deng, C. Surface Modification of PES Ultrafiltration Membrane by Polydopamine Coating and Poly(ethylene glycol) Grafting: Morphology, Stability, and Anti-fouling. *Desalination* **2014**, *344*, 422−430.
(36) Le-Clech, P.; Chen, V.; Fane, T. A. G. Fouling in Membrane Bioreactors used in Wastewater Treatment. *J. Membr. Sci.* **2006**, *284*, 17−53.
(37) Ho, C.; Zydney, A. A Combined Pore Blockage and Cake Filtration Model for Protein Fouling during Microfiltration. *J. Colloid Interface Sci.* **2000**, *232*, 389−399.
(38) Wang, X.; Jiang, Z.; Shi, J.; Zhang, C.; Zhang, W.; Wu, H. Dopamine-modified Alginate Beads Reinforced by Cross-Linking via Titanium Coordination or Self-polymerization and Its Application in Enzyme Immobilization. *Ind. Eng. Chem. Res.* **2013**, *52*, 14828−14836.
(39) De Kerchove, A. J.; Elimelech, M. Formation of Polysaccharide Gel Layers in the Presence of Ca^{2+} and K^{+} Ions: Measurements and Mechanisms. *Biomacromolecules* **2007**, *8*, 113−121.
(40) De Kerchove, A. J.; Elimelech, M. Structural Growth and Viscoelastic Properties of Adsorbed Alginate Layers in Monovalent and Divalent Salts. *Macromolecules* **2006**, *39*, 6558−6564.
(41) Bajpai, S. K.; Sharma, S. Investigation of Swelling/degradation Behaviour of Alginate Beads Crosslinked with Ca^{2+} and Ba^{2+} Ions. *React. Funct. Polym.* **2004**, *59*, 129−140.
(42) Chakrabarty, B.; Ghoshal, A. K.; Purkait, M. K. Effect of Molecular Weight of PEG on Membrane Morphology and Transport Properties. *J. Membr. Sci.* **2008**, *309*, 209−221.
(43) Rao, J.; Yu, A.; Shao, C.; Zhou, X. Construction of Hollow and Mesoporous ZnO Microsphere: A Facile Synthesis and Sensing Property. *ACS Appl. Mater. Interfaces* **2012**, *4*, 5346−5352.
(44) Seifert, D. B.; Phillips, J. a. Porous Alginate - Poly(ethylene glycol) Entrapment System for the Cultivation of Mammalian Cells. *Biotechnol. Prog.* **1997**, *13*, 569−576.

DOI: 10.1021/acsami.5b05529
ACS Appl. Mater. Interfaces 2015, 7, 17682−17691